Supporting information for

Equivalent chemical substitution in double-double perovskite-type ALaLiTeO$_6$:Mn^{4+} (A = Ba^{2+}, Sr^{2+}, Ca^{2+}) phosphors enabling wide range crystal field strength regulation and efficient far-red emission

Jinmei Huang,[a] Pengfei Jiang,*[a] Zien Cheng,[a] Jie Qin,[a] Rihong Cong,[a] and Tao Yang*[a]

[a] College of Chemistry and Chemical Engineering, Chongqing University, Chongqing 401131, China

*Corresponding authors: pengfeijiang@cqu.edu.cn; taoyang@cqu.edu.cn.

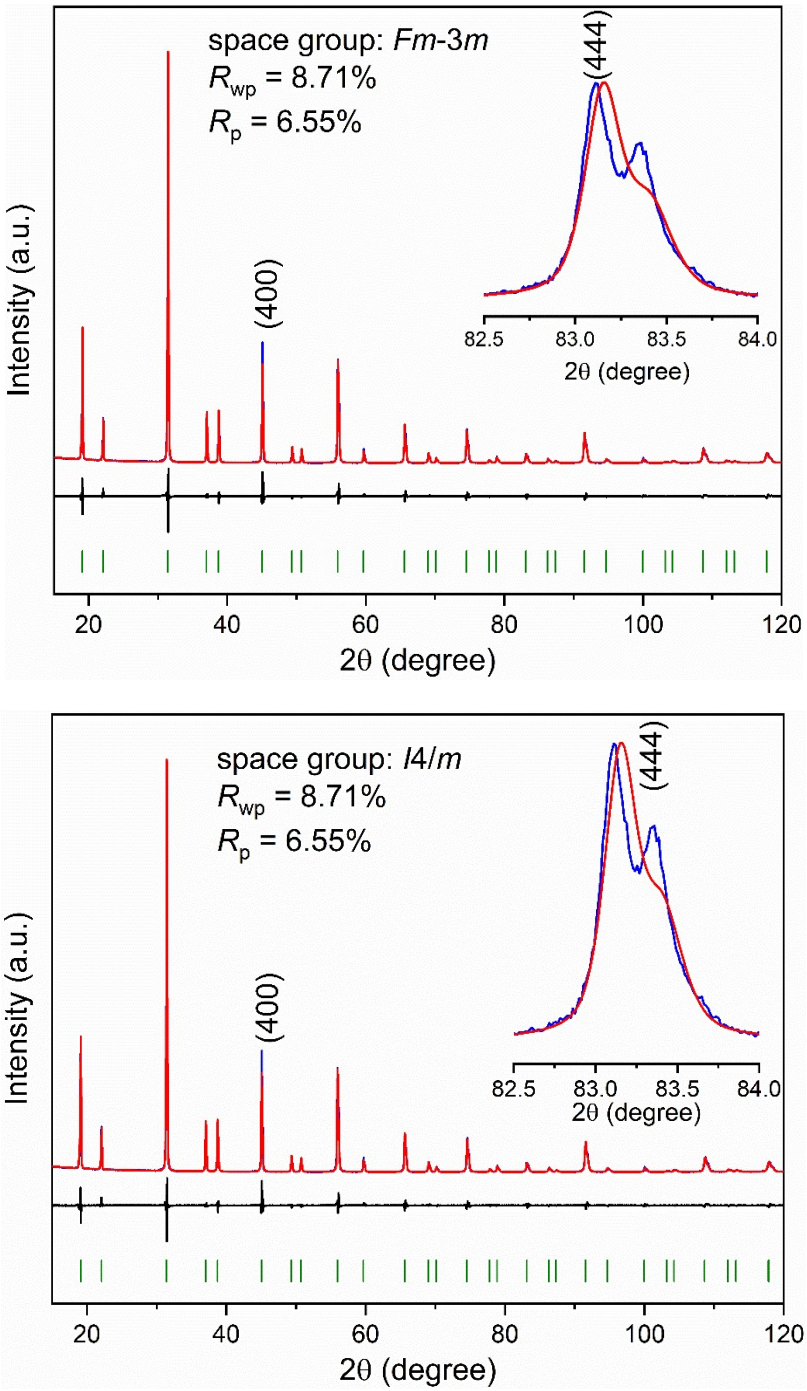

Fig. S1 Rietveld refinement patterns for $BaLaLiTeO_6$:0.015Mn^{4+} using *Fm*-3*m* and *I*4/*m* models. The blue, red, and black solid lines represent the observed, calculated, and differences between the former two. The expected Bragg peak positions are given as green bars at the bottom of the pattern. The insets show the positional discrepancy of the (444) reflection.

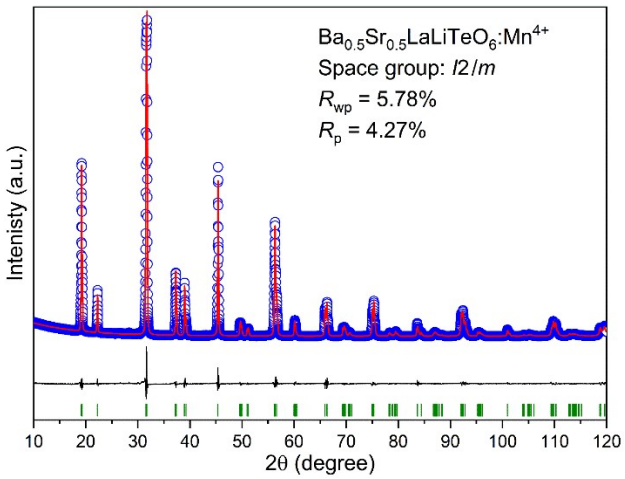

Fig. S2 Rietveld refinement plots of PXRD data for $Ba_{0.5}Sr_{0.5}LaLiTeO_6$:0.015$Mn^{4+}$. The blue circles, red solid lines and black solid lines represent the observed, calculated, and differences between the former two. The expected Bragg peak positions are given as green bars at the bottom of the pattern.

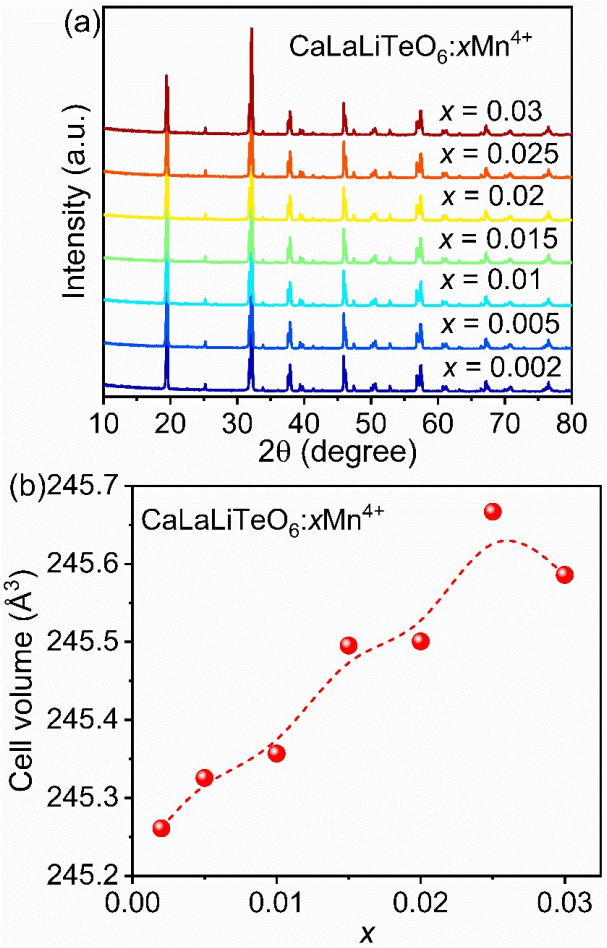

Fig. S3 (a) PXRD patterns for $CaLaLiTeO_6$:*x*Mn^{4+} (*x* = 0.002, 0.005, 0.01, 0.015, 0.02, 0.025, and 0.03). (b) The evolurtion of unit cell volume of $CaLaLiTeO_6$:*x*Mn^{4+} as a function of Mn^{4+}-content (*x*).

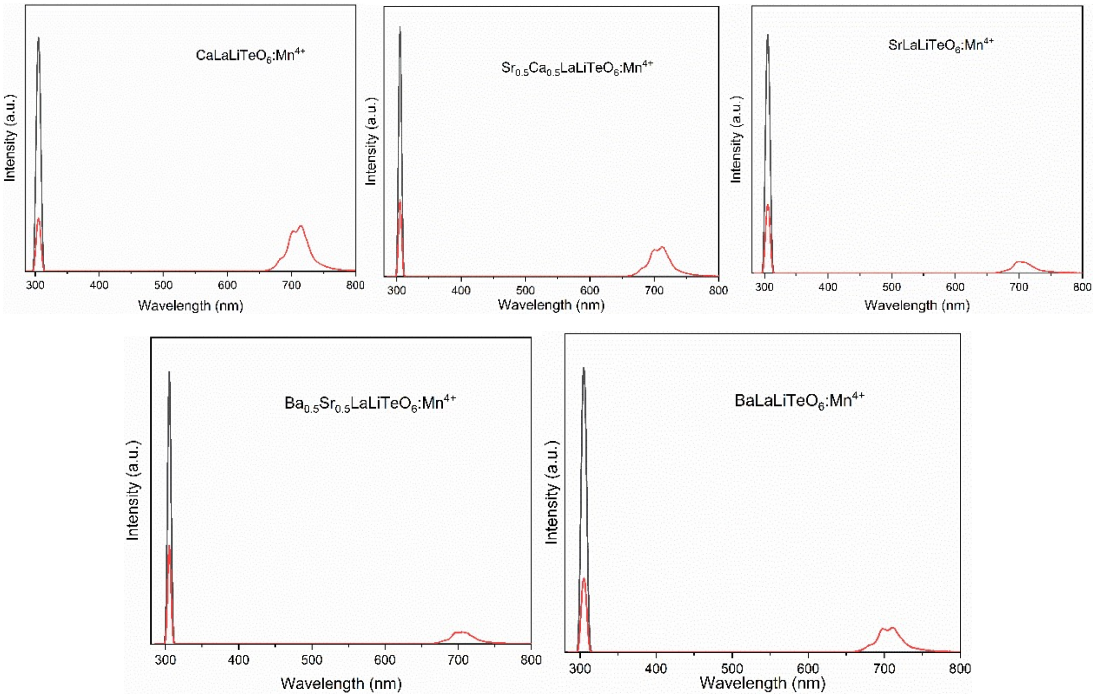

Fig. S4 The optical spectra of ALaLiTeO$_6$:Mn^{4+} (A = Ba, Ba$_{0.5}$Sr$_{0.5}$, Sr, Sr$_{0.5}$Ca$_{0.5}$, and Ca) phosphors recorded by the quantum efficiency system under the excitation wavelength of 305 nm. The black lines in the figures represents the reflectance of the $BaSO_4$ standard.

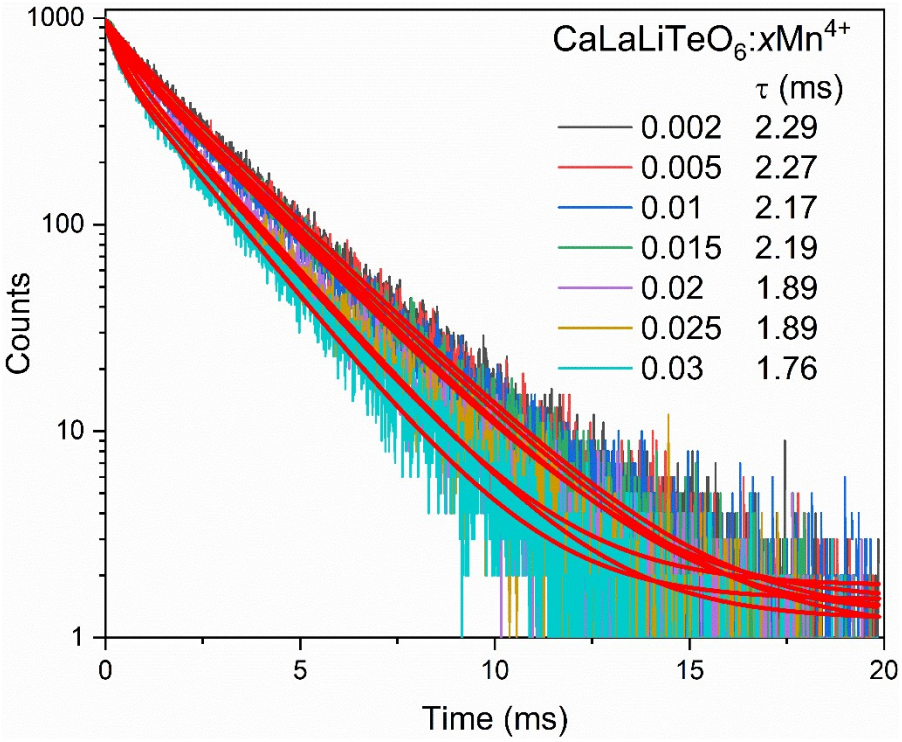

Fig. S5 Room-temperature time-resolved decay curves for CaLaLiTeO$_6$:xMn^{4+} (x = 0.002, 0.005, 0.01, 0.015, 0.02, 0.025, and 0.03). The red solid line is the fitted pattern using a bi-exponential fuhction. The calculated average lifetimes are also presented in the pattern.

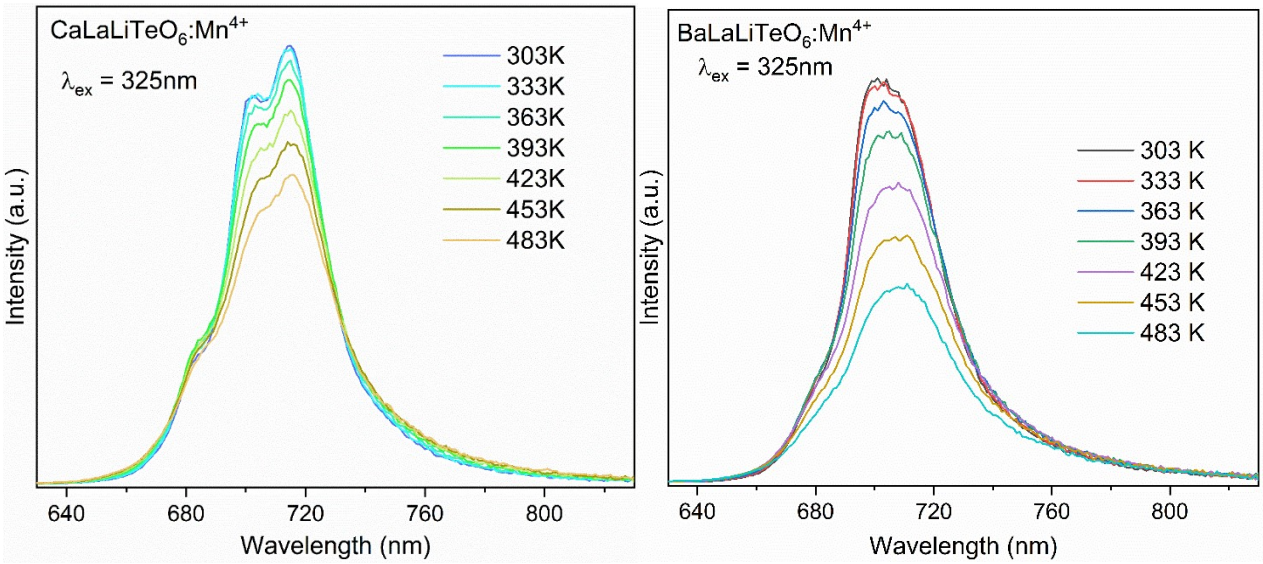

Fig. S6 Temperature-dependent photoluminescence spectra of ALaLiTeO$_6$:Mn^{4+} (A = Ba, and Ca) collected in over the temperature range of 303-483 K.

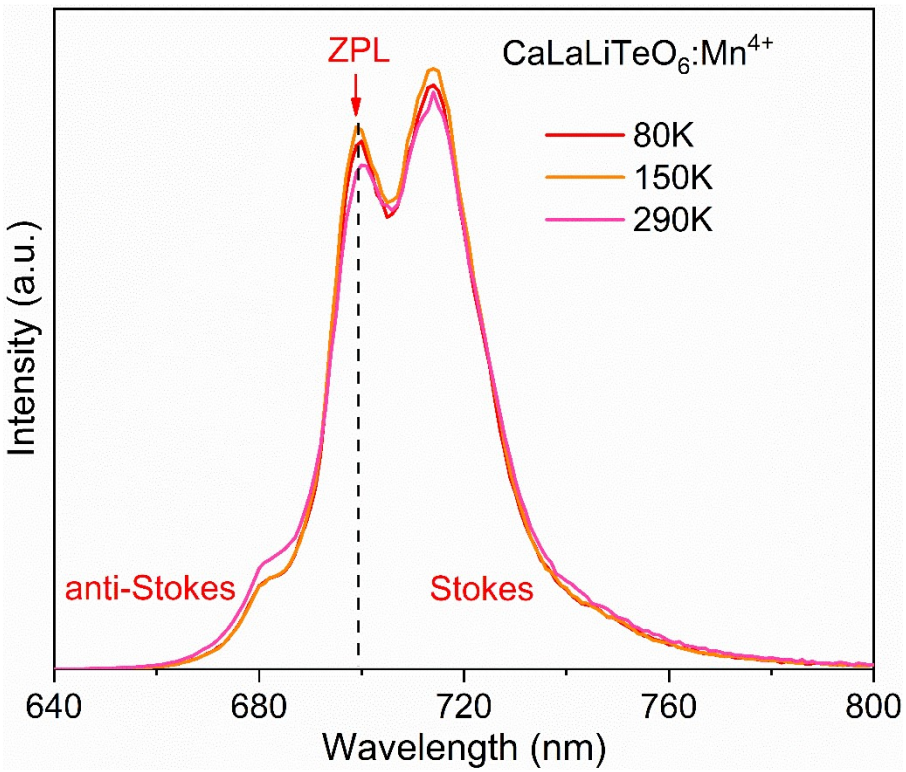

Fig. S7 The PL spectra for CaLaLiTeO$_6$:Mn^{4+} recorded at 290, 150, and 80 K.

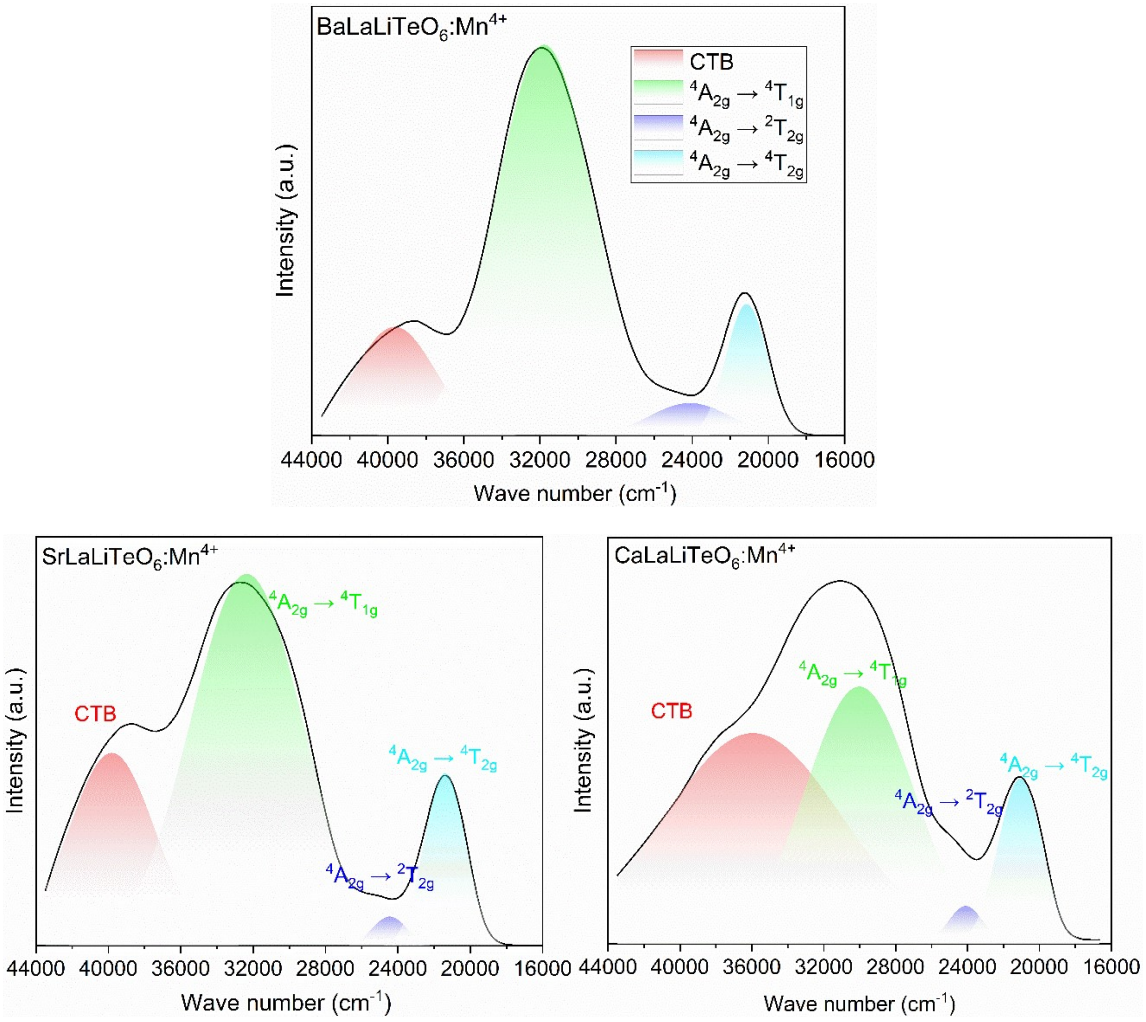

Fig. S8 Gaussian deconvolution patterns of the PLE spectra of ALaLiTeO$_6$:Mn^{4+} (A = Ba, Sr, Ca).

Table S1. Atomic Coordinates, Occupancies, Isotropic Thermal Displacement Factors for ALaLiTeO$_6$:Mn^{4+} (A = Ba$_{0.5}$Sr$_{0.5}$, Sr$_{0.5}$Ca$_{0.5}$) Obtained from Rietveld Refinements against X-ray Diffraction Data.

A = Ba$_{0.5}$Sr$_{0.5}$	site	x	y	z	*sof.*	$B_{iso.}$ (Å)
Ba/Sr/La	4i	0.4990(4)	0	0.2494(2)	0.25/0.25/0.5	0.68(2)
Li	2a	0	0	0	1	1.5(3)
Te	2d	0	0	0.5	1	0.34(2)
O1	4i	0.969(3)	0	0.264(2)	1	1.0(3)
O2	8j	0.275(2)	0.255(2)	0.042(1)	1	1.0(2)
A = Sr$_{0.5}$Ca$_{0.5}$	site	x	y	z	*sof.*	$B_{iso.}$ (Å)
Sr/Ca/La	4e	0.7508(3)	0.4724(1)	0.0014(4)	0.25/0.25/0.5	0.65(2)
Li	2d	0.5	0	0	1	1.0(4)
Te	2a	0	0	0	1	0.20(2)
O1	4e	0.946(2)	0.729(2)	0.210(2)	1	0.57(6)
O2	4e	0.756(2)	0.0103(9)	0.926(2)	1	0.57(6)
O3	4e	0.970(2)	0.208(2)	0.266(2)	1	0.57(6)